Surface & Coatings Technology 483 (2024) 130783

Contents lists available at ScienceDirect

Surface & Coatings Technology

journal homepage: www.elsevier.com/locate/surfcoat

Influence of Cr + Si content variation on cutting behavior of TiAlCrSiN HPPMS coatings

K. Bobzin, C. Kalscheuer, M. Tayyab *

Surface Engineering Institute, RWTH Aachen University, Kackertstraße 15, 52072 Aachen, Germany

ARTICLE INFO

Keywords:
PVD
TiAlCrSiN
HPPMS
Nanocomposite coating
Cutting performance

ABSTRACT

As high power pulse magnetron sputtering (HPPMS) technology is becoming popular in cutting tool industry, the development of nanocomposite coating systems such as TiAlCrSiN with this technology presents a new research avenue. Here, the combined effect of Cr and Si contents on properties and cutting behavior of high Al content TiAlCrSiN HPPMS coatings needs further investigation. For this purpose, three HPPMS coatings with Al/Ti ratio x = 1.4–1.5 and varying Cr + Si content, namely $(Ti_{28}Al_{40}Cr_{16}Si_{16})N$, $(Ti_{30}Al_{43}Cr_{17}Si_{10})N$ and $(Ti_{36}Al_{54}Cr_5Si_5)N$, were deposited on cemented carbide substrates. In addition to basic characterization, the fracture behavior of the coatings was characterized by scratch tests. The cutting behavior of the coated inserts was exemplarily investigated during dry cutting of normalized medium carbon steel C45 with cutting speed v_c = 80 m/min, feed rate f = 0.12 mm and cutting depth a_p = 0.8 mm. The tool damage over the cutting time of t_c = 35–40 min, as per the tool condition, was observed using light microscopy. Moreover, the damage mechanisms were analyzed in detail at the end of the cutting test using scanning electron microscopy. All coatings showed comparable indentation hardness H_{IT} and indentation modulus E_{IT}. However, an increased Cr + Si content amplified the brittle fracture of the coating under sliding load of scratch test. Moreover, the workpiece material C45 showed a higher adhesion tendency to cutting insert with high Cr + Si content TiAlCrSiN coatings during cutting tests. The tool wear and built-up edge formation increased due to the combined effect of workpiece adhesions and amplified brittle fracture of the coating at considered cutting speed. On the other hand, the inserts with low Cr + Si content coating exhibited better cutting performance and reduced built-up edge formation based on the improved fracture behavior of the coating and lower adhesion tendency of workpiece material to the corresponding coated insert.

1. Introduction

Nitride hard coatings developed using physical vapor deposition (PVD) is an established solution to improve service life of cutting tools. These coatings can be deposited using different PVD process variants such as cathodic arc evaporation, direct current magnetron sputtering (dcMS), high power pulse magnetron sputtering (HPPMS), etc. Recently, HPPMS has become popular in cutting tool industry due to its process-driven advantages compared to other variants [1]. Depending on process parameters and target material, very short pulses of high power may lead to increased ionization of pulsed plasma [2,3]. This may result in homogenous distribution of the coating thickness on flank and rake face of the tool [4] along with improved adhesion between coating and substrate [5].

TiN, TiAlN and TiAlSiN are among the most widely used coating systems for cutting tools. These coatings may increase the resistance against abrasive and adhesive wear as well as oxidation-based tool damage. Addition of Al and Cr in TiN matrix have shown to form dense aluminum oxide and chromium oxide layers to improve the overall oxidation stability of the resulting coating system [6]. Moreover, due to its smaller atomic radius compared to Ti, Al addition can increase the lattice distortion and resultantly hardness of the coatings. Incorporation of Si in TiN leads to formation of an amorphous Si_3N_4 phase in the coating. The amorphous phase inhibits the growth of TiN grains limiting the grain size [7]. Hence, the TiSiN system comprises of nanocomposite structure with TiN nanograins embedded in an amorphous Si_3N_4 matrix. This nanocomposite structure may lead to increased hardness and crack resistance of the coating [7,8]. Moreover, Si addition may also improve thermal stability of the coating [9]. As cutting tools are subjected to thermomechanical stress collective during application, the above

* Corresponding author.
E-mail address: tayyab@iot.rwth-aachen.de (M. Tayyab).

https://doi.org/10.1016/j.surfcoat.2024.130783
Received 14 December 2023; Received in revised form 14 March 2024; Accepted 9 April 2024
Available online 15 April 2024

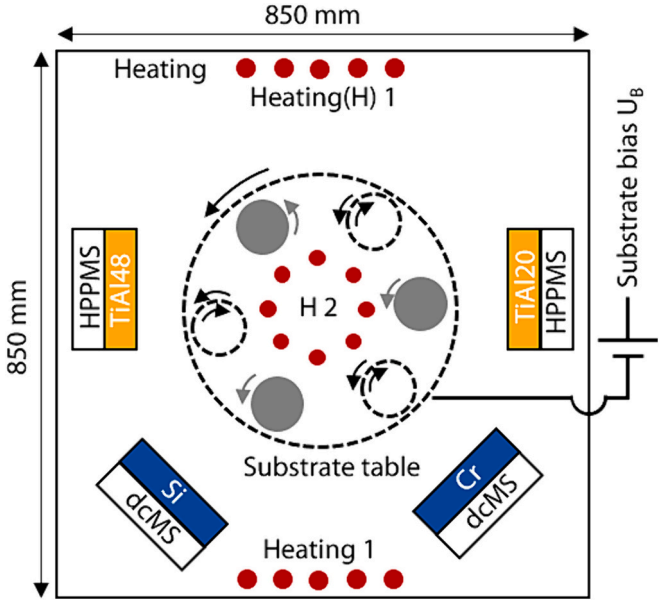

Fig. 1. Schematic of CC800/9 HPPMS coating chamber with target configuration.

discussed coating properties become particularly relevant to improve tool service life. The advantages of Al, Cr and Si addition in TiN can potentially be combined in form of TiAlCrSiN coating system. Previous investigations involving this coating system have shown encouraging results in terms of oxidation behavior [10], thermal stability [11] and tribological behavior of the coating using model tests [12]. Moreover, in [13,14] the influence of deposition parameters such as substrate bias and pulse frequency on cutting performance of coated milling tools against powder metallurgical high speed steel HS6–5-3C were investigated. The coatings studied in these investigations were deposited by a hybrid process combining dcMS and HPPMS. The development of nanocomposite TiAlCrSiN coatings with high HPPMS content for cutting tool applications presents a new research avenue. Hereby, the influence of coating chemical composition, especially in terms of Cr and Si contents, on cutting performance of the coated tool needs further investigations.

The main aim of the study lies in analyzing the effect of Cr + Si content on properties of HPPMS TiAlCrSiN coatings and resulting cutting behavior of coated cutting inserts. For this purpose, three high Al content TiAlCrSiN coatings with varying Cr + Si contents are deposited predominantly using HPPMS. Other than basic characterization, scratch tests are carried out to study the fracture behavior of the coatings under sliding load. The influence of coating composition on cutting behavior of the coated inserts is exemplarily studied with the help of cutting tests involving longitudinal turning of C45 steel. The wear and damage behavior of the cutting inserts is analyzed using light microscopy and scanning electron microscopy (SEM).

2. Experimental methods

2.1. Coating deposition

For coating deposition, an industrial coating unit CC800/ HPPMS from CemeCon AG, Wuerselen, Germany, was used. The coatings under investigation were deposited using two HPPMS and two dcMS cathodes with same target configuration, see Fig. 1. The TiAl20 and TiAl48 targets corresponding to major elements of the coating system were installed on HPPMS cathodes. These targets consisted of Ti base with 20 and 48 Al plugs, respectively. Pure Si and Cr targets were installed on two dcMS cathodes. The substrate samples were subjected to a three-fold rotation during deposition, whereby the substrate table was rotated at a speed $n_{Table} = 1\ min^{-1}$.

Table 1
Process parameters used for depositing TiAlCrSiN coatings with varying Cr + Si contents.

Process parameters	Unit	Value
Pressure p	mPa	520
Argon flow j_{Ar}	sccm	200
Nitrogen flow j_{N2}	sccm	Pressure controlled
Heating power on sides P_{H1}	kW	8
Heating power in centre P_{H2}	kW	4
Substrate bias U_B	V	−80
Average power HPPMS P_{HPPMS}	kW	7.0
Power dcMS-Si $P_{dcMS-Si}$	**kW**	**1.5/1.0/0.6**
Power dcMS-Cr $P_{dcMS-Cr}$	**kW**	**0.8/0.8/0.3**
Pulse frequency f	Hz	2000
Pulse duration t_{on}	µs	60

The process parameters for all three variants are shown in Table 1. The coating architecture consisted of TiAlCrN bond layer followed by the TiAlCrSiN top layer. The dcMS cathodes were operated with relatively low average power compared to HPPMS cathodes to deposit coatings with high Al and HPPMS content. Cr + Si content of the investigated coatings was varied by changing the power of dcMS-Si and dcMS-Cr cathodes. Coating with high Cr + Si content was deposited with $P_{dcMS-Si} = 1.5$ kW and $P_{dcMS-Cr} = 0.8$ kW. For second variant, power of dcMS cathode with Si target was reduced to $P_{dcMS-Si} = 1.0$ kW and power of dcMS cathode with Cr target was kept same. For third variant with low Cr + Si content, power of used dcMS cathodes was reduced to $P_{dcMS-Si} = 0.6$ kW and $P_{dcMS-Cr} = 0.3$ kW. Remaining process parameters for the three coating processes were kept constant.

2.2. Coating and compound properties

For investigation of coating and compound properties, TiAlCrSiN coatings were deposited on cemented carbide indexable inserts SNUN 120412 THM of grade HB10, Kennametal Widia Produktions GmbH & Co. KG, Essen, Germany. Cross-section images captured with Zeiss DSM 982 Gemini SEM, Jena, Germany, were used to study the coating morphology and thickness. Chemical composition of the coatings was measured by electron probe microanalysis (EPMA) method using JEOL JXA-8530, Jeol, Tokyo, Japan. SEM and EPMA investigations were carried out at Central Facility for Electron Microscopy (GFE), RWTH Aachen University, Aachen, Germany. Average line roughness Ra was measured with confocal laser scanning microscopy (CLSM), VKX 210, Keyence Corporation, Osaka, Japan. Phase composition was studied by X-ray diffraction method (XRD) using X-ray diffractometer 3003 from GE Energy GmbH, Ratingen, Germany. The measurements were carried out using Cu-Kα radiation at voltage U = 40 kV, current $I = 40$ mA, wavelength $\lambda = 0.1540598$ nm, step size $s = 0.01°$, step time $t = 10$ s, incidence angle $\omega = 2°$ and diffraction angle $2\theta = 20° - 80°$. Indentation hardness H_{IT} and indentation modulus E_{IT} of the coatings were measured by nanoindentation according to ISO 14577-1:2015. A Berkovich shaped diamond indenter, having a nominal radius $r = 150$ nm, installed on Triboindenter TI 950, Bruker Corporation, Billerica, Massachusetts, USA, was used for this purpose. 50 measurements with maximum indentation force $F_{max} = 8$ mN were carried out for each variant. The resulting force-displacement data was used to calculate average H_{IT} and E_{IT} values as per Oliver and Pharr method [15]. For calculation, Poisson's ratio $\nu = 0.25$ was assumed. The adhesion between coating and substrate was characterized by Rockwell C indentation test according to DIN 4856 using HP100 Rockwell tester, KNUTH Machine Tools GmbH, Wasbek, Germany. The tests were carried out with a diamond indenter having cone angle $\Theta = 120°$ and normal force $F \approx 588.4$ N. Indent imprints were analyzed by CLSM to determine the adhesion strength category (HF). Fracture behavior of the coatings under sliding load was

Table 2
Coating thickness s, average line roughness Ra, chemical composition, indentation hardness H_{IT}, indentation modulus E_{IT} and adhesion strength category HF of TiAlCrSiN coatings.

Sample ID	4696	4698	4809
s [µm]	2.5	2.5	2.7
Ra [µm]	0.07	0.09	0.07
Ti [at. %]	13.2	14.1	16.8
Al [at. %]	19.1	20.5	25.0
Cr [at. %]	7.7	8.0	2.5
Si [at. %]	7.5	4.8	2.5
N [at. %]	52.5	52.6	53.2
H_{IT} [GPa]	28.0 ± 3.2	29.2 ± 2.1	31.6 ± 2.4
E_{IT} [GPa]	367.5 ± 34.0	365.9 ± 18.5	385.6 ± 27.7
HF [−]	2	2	1
Coating designation	$(Ti_{28}Al_{40}Cr_{16}Si_{16})N$	$(Ti_{30}Al_{43}Cr_{17}Si_{10})N$	$(Ti_{36}Al_{54}Cr_5Si_5)N$

studied using constant force scratch tests according to DIN EN ISO 20502:2016. The tests were carried out with a sliding velocity $v_s = 250$ mm/min and normal force starting from F = 10 N till F = 90 N with ΔF = 10 N. A diamond indenter installed on Scratch Tester HPG 200/2, Gesellschaft für Fertigungstechnik und Entwicklung Schmalkalden e.V., Schmalkalden, Germany, was used for this purpose. Scratch tracks were analyzed for cracks and coating delamination using CLSM.

2.3. Cutting tests

In order to exemplarily study the cutting behavior of the coatings, cutting tests were carried out. For this purpose, cemented carbide inserts CNMG 120408-QM H13A from Sandvik Coromant, Sandviken, Sweden, were coated as mentioned in Section 2.1. The cutting inserts had a corner radius $r_\varepsilon = 0.79$ mm, main clearance angle $\alpha = 0°$ and wedge angle $\beta = 80°$. The cutting process involved CNC longitudinal turning of C45 steel in normalized state on SB-CNC machine, Spinner AG, CNC Präzisionsmaschinen, Kleinandelfingen, Switzerland. The tests were carried out at Feinmechanik Mehr GmbH & Co. KG, Aachen, Germany, with cutting velocity $v_c = 80$ m/min, cutting depth $a_p = 0.8$ mm and feed rate f = 0.12 mm under dry cutting condition. The tool wear progress was analyzed after cutting intervals Δt_c = 5–7 min using light microscope, Zeiss Axio Imager, Carl Zeiss Microscopy Deutschland GmbH, Oberkorchen, Germany. For tool life criteria, a maximum cutting time t_c = ~35–40 min, as per tool condition was defined. Two cutting tests were carried out for each coated variant. The cutting inserts, at the end of cutting tests, were analyzed in detail using SEM to determine the underlying tool damage mechanisms. Desktop SEM Phenom XL from Thermo Fischer Scientific, Eindhoven, Netherland, was used for this purpose.

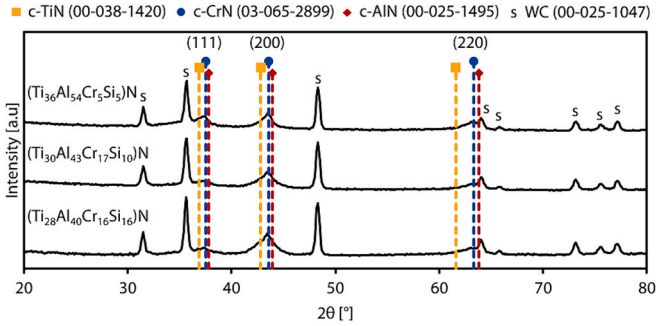

Fig. 3. XRD results of TiAlCrSiN coatings deposited on WC-Co substrates.

3. Results

3.1. Coating characterization

Coating characterization results such as chemical composition, thickness s, average line roughness Ra, indentation hardness H_{IT} and indentation modulus E_{IT} and adhesion strength class (HF) are summarized in Table 2. The investigated coatings had a comparable thickness and surface roughness. All investigated coatings had an almost similar nitrogen content. The reduction in Cr + Si content was compensated with addition of Al and Ti. However, an overall Al to Ti ratio of $x_{Al/Ti}$ = 1.4–1.5 was almost constant in all variants. The coatings are designated after excluding the atomic percentage of nitrogen for an intuitive representation of remaining coating elements.

H_{IT} and E_{IT} values did not differ significantly for the considered variants. $(Ti_{36}Al_{54}Cr_5Si_5)N$ showed a slight increase in indentation hardness H_{IT} compared to $(Ti_{28}Al_{40}Cr_{16}Si_{16})N$. However, indentation modulus E_{IT} of all variants is comparable. Albeit the high Si content and presumably an increased amorphous content, indentation hardness H_{IT} for $(Ti_{28}Al_{40}Cr_{16}Si_{16})N$ did not reduce significantly. Therefore, TiAlCrSiN coatings deposited with HPPMS technology may well be explored further to develop high Si content coatings having high hardness. The adhesion between the coating and substrate for all variants was categorized within an acceptable range of HF1-HF2 as per DIN 4856. Moreover, the coatings showed a non-columnar dense morphology, see Fig. 2.

XRD analysis results are shown in Fig. 3. The XRD spectrum consisted of strong diffraction peaks attributed to cemented carbide substrate. However, weak (111, 200, 220) diffraction peaks could be associated to face centered cubic (fcc) TiN, CrN or AlN phases belonging to the coating. Moreover, no peaks belonging to silicon containing cubic phases were observed. This indicates that silicon may preferably form amorphous phases with nitrogen. As previously observed in [18], these results points towards a formation of nanocomposite structure containing cubic (Ti, Al, Cr)N nanocrystals embedded in Si-based amorphous matrix.

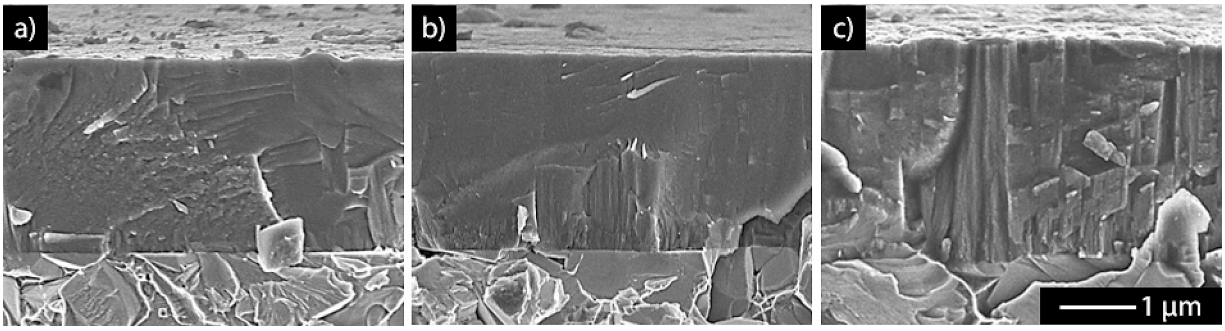

Fig. 2. SEM cross-section images of (a) $(Ti_{28}Al_{40}Cr_{16}Si_{16})N$, (b) $(Ti_{30}Al_{43}Cr_{17}Si_{10})N$ and (c) $(Ti_{36}Al_{54}Cr_5Si_5)N$ coatings.

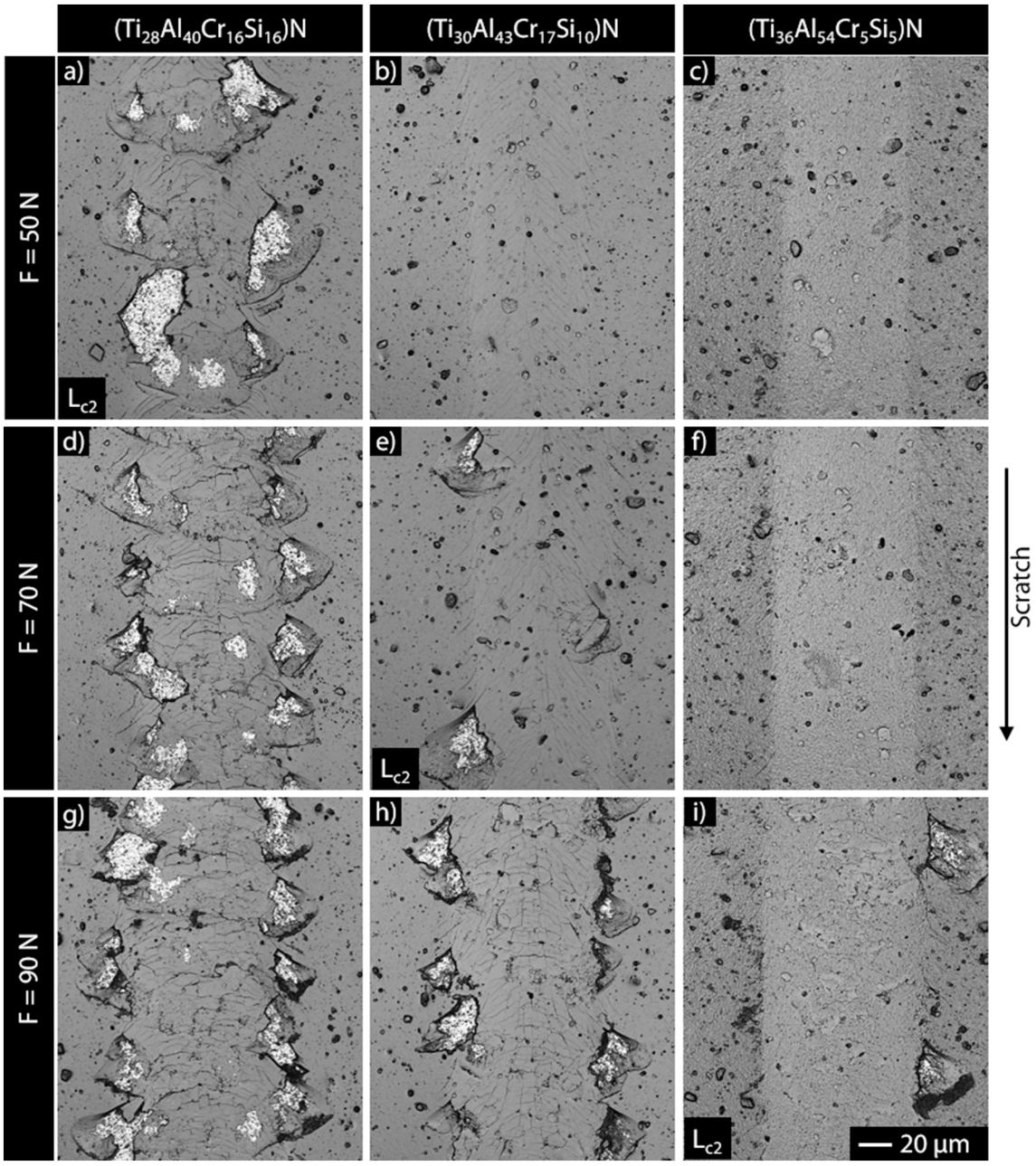

Fig. 4. Scratch tracks for the investigated TiAlCrSiN coatings at normal load (a-c) F = 50 N, (d-f) F = 70 N and (g-i) F = 90 N.

3.2. Fracture behavior

The fracture behavior of the coatings was studied using constant force scratch tests. As the coatings were deposited on same substrate material with comparable interlayer and overall coating thickness, the influence of these factors on fracture behavior of the coating at considered loads could be considered alike for all variants. In scratch tests, critical normal load L_{c2} denotes the starting normal load for onset of coating fracture and delamination at scratch edges. Hence, fracture behavior of the coatings is compared at the corresponding critical normal loads L_{c2} to analyze the influence Cr + Si content of the coating. Fig. 4 shows images of scratch tracks at observed critical normal loads L_{c2} for the three coatings. $(Ti_{28}Al_{40}Cr_{16}Si_{16})N$ showed an earlier initiation of coating fracture, i.e. at F = 50 N, compared to the other two variants. $(Ti_{30}Al_{43}Cr_{17}Si_{10})N$ eventually started delaminating at F = 70 N. $(Ti_{36}Al_{54}Cr_5Si_5)N$ showed highest resistance against fracture and delamination under sliding load. The coating first showed cohesive damage and resulting fracture around scratch edges at F = 90 N. At F = 90 N, $(Ti_{28}Al_{40}Cr_{16}Si_{16})N$ and $(Ti_{30}Al_{43}Cr_{17}Si_{10})N$ showed significantly more fracture areas compared to $(Ti_{36}Al_{54}Cr_5Si_5)N$. Hence, an increase in Cr + Si content of the coating decreased the resistance of the coated compound against cohesive damage and amplified the brittle fracture of the coating. This is presumably based on the increased Si-based amorphous content and resulting change in residual stress state of the coating at higher Cr + Si content. As previously observed in case of TiAlSiN [16] and CrAlSiN [17], an increase in Si content beyond $x_{Si} > \sim 5$ at. % may reduce the compressive residual stresses of the coating. A reduction in compressive residual stresses accompanied by increased amorphous phase may result in decreased fracture toughness of TiAlCrSiN coatings.

3.3. Cutting behavior

The wear progress on flank face of the tool captured at comparable cutting intervals for investigated coated cutting inserts is exemplarily

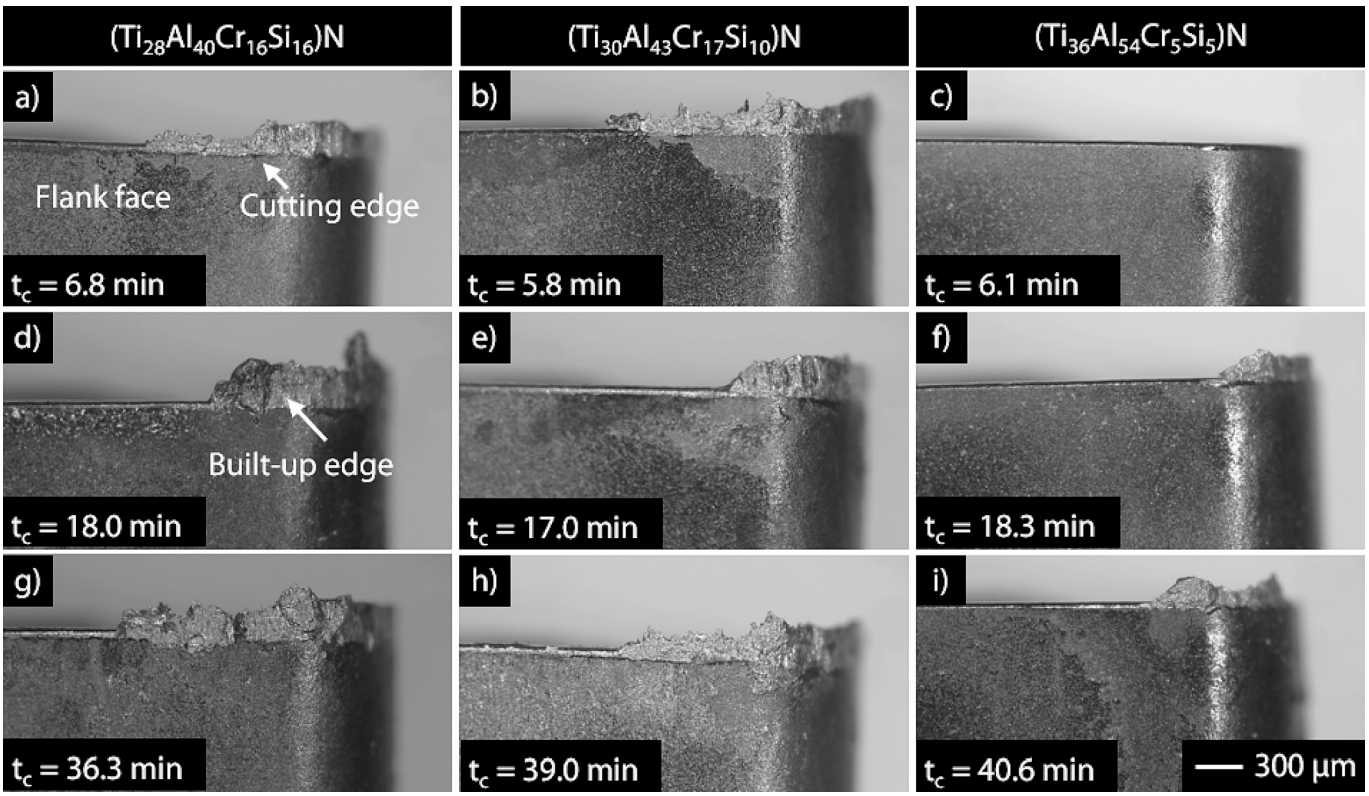

Fig. 5. Wear progress on flank face of TiAlCrSiN coated cutting inserts at varying cutting times t_c representing (a-c) start, (d-f) middle and (g-h) end of cutting test.

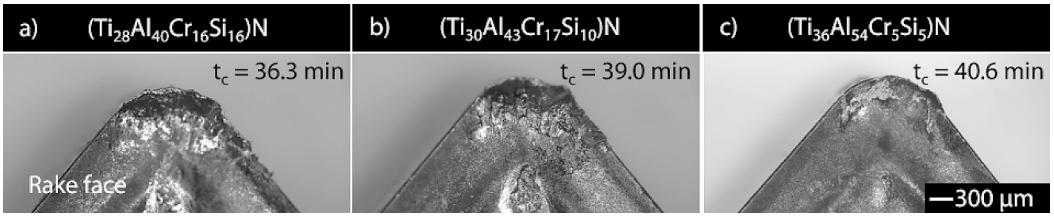

Fig. 6. Wear on the rake face of cutting inserts coated with (a) $(Ti_{28}Al_{40}Cr_{16}Si_{16})N$, (b) $(Ti_{30}Al_{43}Cr_{17}Si_{10})N$ and (c) $(Ti_{36}Al_{54}Cr_5Si_5)N$ coatings at the end of cutting test.

shown in Fig. 5. The results were found to be repeatable for both cutting tests of each coated variant. Fig. 5(a-c) display the tool wear after first cutting interval. $(Ti_{28}Al_{40}Cr_{16}Si_{16})N$ and $(Ti_{30}Al_{43}Cr_{17}Si_{10})N$ coated inserts showed a strong tendency towards built-up edge formation. However, $(Ti_{36}Al_{54}Cr_5Si_5)N$ coated insert showed a better resistance to formation of built-up edge. This trend continued as the cutting time increased until the cutting edge was deemed to have reached the end of its service life, see Fig. 5 (d-i). The cutting insert coated with low Cr + Si content showed an increased resistance to built-up edge formation and resultantly better cutting behavior for the considered cutting parameters compared to other two variants. Fig. 6 shows the wear condition on the rake face of coated inserts at the end of cutting test. Again, $(Ti_{36}Al_{54}Cr_5Si_5)N$ coated insert exhibited a reduced abrasive wear and coating delamination compared to the variants with $(Ti_{28}Al_{40}Cr_{16}Si_{16})N$ and $(Ti_{30}Al_{43}Cr_{17}Si_{10})N$ coatings.

3.4. Damage analysis

SEM-based damage analysis of cutting inserts in form of energy dispersive X-ray (EDX) mappings of cutting edge and flank face is shown in Fig. 7. Coating, substrate and workpiece material are represented by the EDX maps of their corresponding major elements, see Figs. 7(a), (e) and (i). Ti and Al shown in dark blue and purple colors, respectively, mainly represent the TiAlCrSiN coating. Fe, in yellow color, signify the adhesions from workpiece material on the cutting edge of the insert. Substrate exposure, resulting from coating wear and delamination, is shown in aqua blue color as EDX map of W. Cutting insert with $(Ti_{36}Al_{54}Cr_5Si_5)N$ coating displayed reduced adhesion of workpiece material around the cutting edge compared to the other two variants, see Figs. 7(b), (f) and (j). The increased adhesion of the workpiece material on the coated surface can accelerate tool wear. Hence, cutting inserts with $(Ti_{28}Al_{40}Cr_{16}Si_{16})N$ and $(Ti_{30}Al_{43}Cr_{17}Si_{10})N$ coatings showed an increased substrate exposure resulting from wear or delamination of the coating, see Figs. 7(a), (c), (e), (g), (i) and (k). The built-up edge seems to form on the exposed substrate at the cutting edge. The repeated partial break up and reformation of built-up edge in successive cutting intervals may fast-track coating delamination and overall tool wear. The presence of oxygen, represented in red, was also qualitatively analyzed to characterize any oxidation-based damage of the cutting insert. As apparent in Figs. 7(d), (h) and (i), oxidation is mostly concentrated in the areas consisting of adhesions from the workpiece material. Depending on the cutting parameters, tool and workpiece material the tool may be subjected to temperatures $T > 500$ °C [19] during the cutting process. Hence, as expected, C45 steel adhesions on the tool surface oxidized

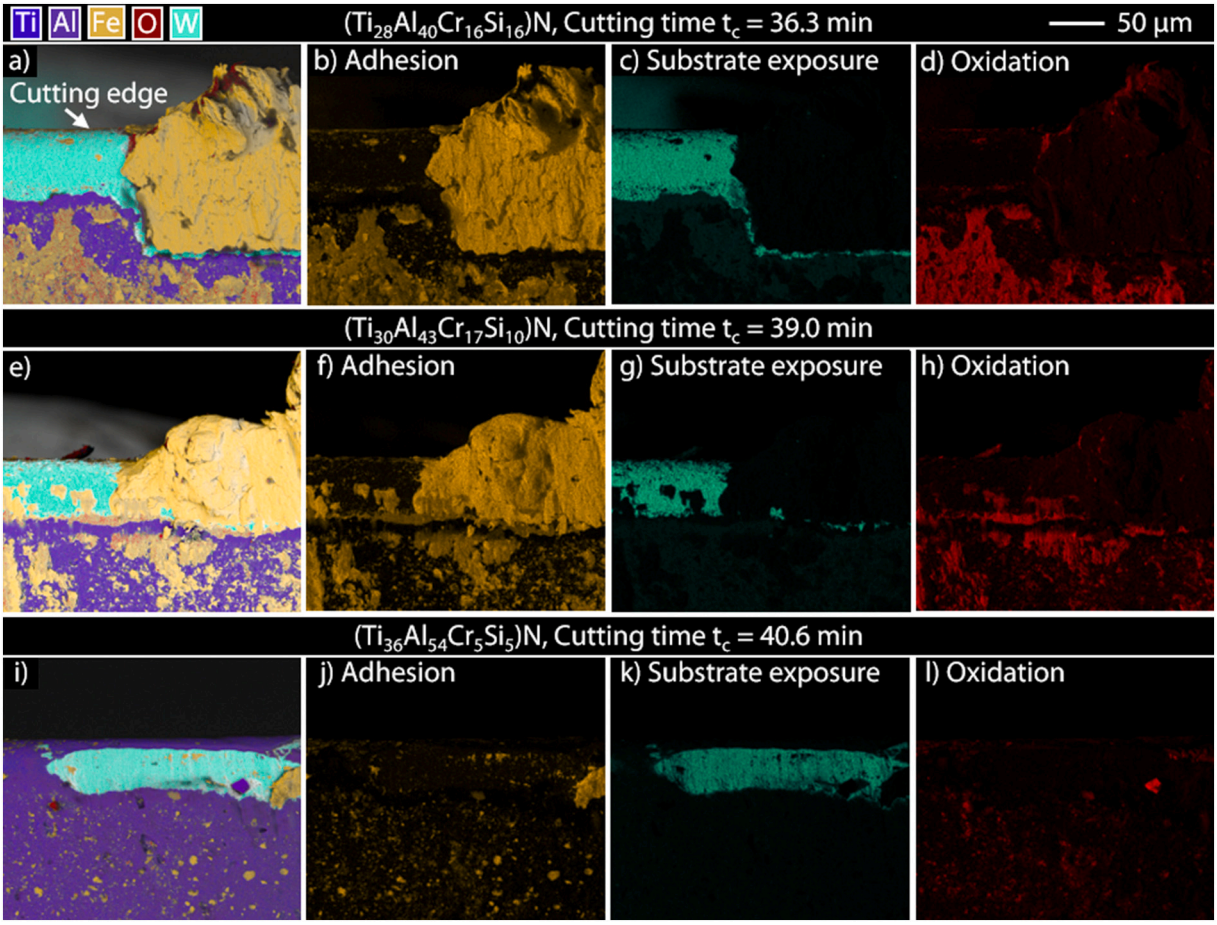

Fig. 7. EDX mappings of flank face of cutting inserts coated with (a-d) $(Ti_{28}Al_{40}Cr_{16}Si_{16})N$, (e-h) $(Ti_{30}Al_{43}Cr_{17}Si_{10})N$ and (i-l) $(Ti_{36}Al_{54}Cr_5Si_5)N$ coatings after cutting test.

during the cutting process. Although, the coated inserts were subjected to a dry cutting condition, no oxidation of coating is apparent in present case for all variants. Therefore, any contribution from coating oxidation to overall tool wear can be ruled out.

4. Conclusion

The current study showed that the Cr + Si content in HPPMS TiAlCrSiN coatings may significantly affect the fracture behavior of the coating and resulting cutting behavior of coated inserts. An increased Cr + Si content may amplify the brittle fracture of the TiAlCrSiN coatings. Moreover, the workpiece material C45 showed a higher adhesion tendency to cutting inserts with high Cr + Si content TiAlCrSiN coatings during cutting tests. The tool wear and built-up edge formation increased due to the combined effect of increased workpiece adhesions and amplified brittle fracture of the coating at considered cutting speed. On the other hand, the inserts with low Cr + Si content coating exhibited better cutting performance and reduced built-up edge formation. This can be attributed to the observed improved fracture behavior of the low Cr + Si content TiAlCrSiN coating and lower adhesion tendency of workpiece material C45 to the corresponding coated insert. The findings provide preliminary guidance on development of nanocomposite high Al content TiAlCrSiN coatings in HPPMS regime for cutting tool applications.

CRediT authorship contribution statement

K. Bobzin: Funding acquisition, Conceptualization, Project administration, Resources, Supervision, Writing – review & editing. **C. Kalscheuer:** Conceptualization, Funding acquisition, Project administration, Supervision, Writing – review & editing. **M. Tayyab:** Conceptualization, Formal analysis, Investigation, Methodology, Visualization, Writing – original draft.

Declaration of competing interest

The authors declare that they have no known competing financial interests or personal relationships that could have appeared to influence the work reported in this paper.

Acknowledgement

The authors gratefully acknowledge the financial support of the German Research Foundation, Deutsche Forschungsgemeinschaft (DFG), within the project BO 1979/99-1.

References

[1] S. Quach, C. Fabian, L. Kretzschmar, M. Hütteneder, T. Schmidle, J. Tanson, M. Schmidt, S. Deutschbauer, Evaluation of the market potential of HiPIMS and advanced coating technologies, Zenodo (1) (2021) 18–19, https://zenodo.org/doi/10.5281/zenodo.4551290.
[2] J. Bohlmark, J. Alami, C. Christou, A.P. Ehiasarian, U. Helmersson, Ionization of sputtered metals in high power pulsed magnetron sputtering, J. Vac. Sci. Technol. A 23 (2005) 18–22, https://doi.org/10.1116/1.1818135.
[3] E. Lewin, D. Loch, A. Montagne, A.P. Ehiasarian, J. Patscheider, Comparison of Al–Si–N nanocomposite coatings deposited by HIPIMS and DC magnetron sputtering, Surf. Coat. Technol. 232 (2013) 680–689, https://doi.org/10.1016/j.surfcoat.2013.06.076.
[4] K. Bobzin, N. Bagcivan, P. Immich, S. Bolz, R. Cremer, T. Leyendecker, Mechanical properties and oxidation behaviour of (Al,Cr)N and (Al,Cr,Si)N coatings for cutting

tools deposited by HPPMS, Thin Solid Films 517 (2008) 1251–1256, https://doi.org/10.1016/j.tsf.2008.06.050.
[5] Q. Ma, L. Li, Y. Xu, J. Gu, L. Wang, Y. Xu, Effect of bias voltage on TiAlSiN nanocomposite coatings deposited by HiPIMS, Appl. Surf. Sci. 392 (2017) 826–833, https://doi.org/10.1016/j.apsusc.2016.09.028.
[6] E. Huber, S. Hofmann, Oxidation behaviour of chromium-based nitride coatings, Surf. Coat. Technol. 68-69 (1994) 64–69, https://doi.org/10.1016/0257-8972(94)90139-2.
[7] S. Vepřek, S. Reiprich, L. Shizhi, Superhard nanocrystalline composite materials: the TiN/Si3N4 system, Appl. Phys. Lett. 66 (1995) 2640–2642, https://doi.org/10.1063/1.113110.
[8] N. Jiang, Y. Shen, Y.-W. Mai, T. Chan, S.C. Tung, Nanocomposite Ti–Si–N films deposited by reactive unbalanced magnetron sputtering at room temperature, Mater. Sci. Eng. B 106 (2004) 163–171, https://doi.org/10.1016/j.mseb.2003.09.033.
[9] J.M. Wheeler, R. Raghavan, V. Chawla, M. Morstein, J. Michler, Deformation of hard coatings at elevated temperatures, Surf. Coat. Technol. 254 (2014) 382–387, https://doi.org/10.1016/j.surfcoat.2014.06.048.
[10] M.-R. Alhafian, N. Valle, J.-B. Chemin, L. Bourgeois, M. Penoy, R. Useldinger, J. Ghanbaja, F. Mücklich, P. Choquet, Influence of Si addition on the phase structure and oxidation behavior of PVD AlTiN and AlTiCrN coatings using high-resolution characterization techniques, J. Alloys Compd. 968 (2023) 171800, https://doi.org/10.1016/j.jallcom.2023.171800.
[11] K. Bobzin, T. Brögelmann, N.C. Kruppe, M. Carlet, Wear behavior and thermal stability of HPPMS (Al,Ti,Cr,Si)ON, (Al,Ti,Cr,Si)N and (Ti,Al,Cr,Si)N coatings for cutting tools, Surf. Coat. Technol. 385 (2020) 125370, https://doi.org/10.1016/j.surfcoat.2020.125370.
[12] W. Schulz, V. Joukov, F. Köhn, W. Engelhart, V. Schier, T. Schubert, J. Albrecht, The behavior of TiAlN and TiAlCrSiN films in abrasive and adhesive Tribological contacts, Coatings 13 (2023) 1603, https://doi.org/10.3390/coatings13091603.
[13] K. Bobzin, T. Brögelmann, N.C. Kruppe, M. Carlet, HPPMS TiAlCrSiN - influence of substrate bias and pulse frequency on cutting performance, Surf. Coat. Technol. 397 (2020) 126056, https://doi.org/10.1016/j.surfcoat.2020.126056.
[14] K. Bobzin, T. Brögelmann, H.J. Maier, T. Heidenblut, C. Kahra, M. Carlet, Influence of residual stresses in hard tool coatings on the cutting performance, J. Manuf. Process. 69 (2021) 340–350, https://doi.org/10.1016/j.jmapro.2021.08.011.
[15] W.C. Oliver, G.M. Pharr, An improved technique for determining hardness and elastic modulus using load and displacement sensing indentation experiments, J. Mater. Res. 7 (1992) 1564–1583, https://doi.org/10.1557/JMR.1992.1564.
[16] W. Tillmann, M. Dildrop, Influence of Si content on mechanical and tribological properties of TiAlSiN PVD coatings at elevated temperatures, Surf. Coat. Technol. 321 (2017) 448–454, https://doi.org/10.1016/j.surfcoat.2017.05.014.
[17] C. Tritremmel, R. Daniel, M. Lechthaler, P. Polcik, C. Mitterer, Influence of Al and Si content on structure and mechanical properties of arc evaporated Al–Cr–Si–N thin films, Thin Solid Films 534 (2013) 403–409, https://doi.org/10.1016/j.tsf.2013.03.017.
[18] K. Bobzin, T. Brögelmann, N.C. Kruppe, M. Carlet, Investigation on the incorporation of oxygen and thermal stability of HPPMS TiAlCrSiON nanolayer coatings, Surf. Coat. Technol. 418 (2021) 127231, https://doi.org/10.1016/j.surfcoat.2021.127231.
[19] F. Klocke, Fertigungsverfahren 1: Zerspanung mit geometrisch bestimmter Schneide, Springer Vieweg, Berlin, 2017, https://doi.org/10.1007/978-3-662-54207-1.